Molecular Structure of 1,5-Diazabicyclo[3.1.0]hexane as Determined by Gas Electron Diffraction and Quantum-Chemical Calculations

Yuri V. Vishnevskiy,*,† Natalja Vogt,† Jürgen Vogt,† Anatolii N. Rykov,‡ Vladimir V. Kuznetsov,§ Nina N. Makhova,§ and Lev V. Vilkov‡

Chemieinformationssysteme, University of Ulm, D-89069 Ulm, Germany, Chemistry Department, Moscow State University, 119992 GSP-2, Leniskiye gori 1, bld. 3, Moscow, Russia, and N. Zelinskiy Institute of Organic Chemistry, Russian Academy of Sciences, 117913, Leninsky pr. 47, Moscow, Russia

Received: February 14, 2008; Revised Manuscript Received: March 21, 2008

The equilibrium molecular structure and conformation of 1,5-diazabicyclo[3.1.0]hexane (DABH) has been studied by the gas-phase electron-diffraction method at 20 °C and quantum-chemical calculations. Three possible conformations of DABH were considered: boat, chair, and twist. According to the experimental and theoretical results, DABH exists exclusively as a boat conformation of C_s symmetry at the temperature of the experiment. The MP2 calculations predict the stable chair and twist conformations to be 3.8 and 49.5 kcal mol^{-1} above the boat form, respectively. The most important semi-experimental geometrical parameters of DABH (r_e, Å and $\angle_e$, deg) are (N1−N5) = 1.506(13), (N1−C6) = 1.442(2), (N1−C2) = 1.469(4), (C2−C3) = 1.524(7), (C6−N1−C2) = 114.8(8), (N5−N1−C2) = 107.7(4), (N1−C2−C3) = 106.5(9), and (C2−C3−C4) = 104.0(10). The natural bond orbital (NBO) analysis has shown that the most important stabilization factor in the boat conformation is the n(N) → σ*(C−C) anomeric effect. The geometry calculations and NBO analysis have been performed also for the bicyclohexane molecule.

Introduction

1,5-Diazabicyclo[3.1.0]hexane (DABH, Figure 1) is the unusual and highly energetic derivative of the diaziridine because *cis*-diaziridines are thermodynamically less stable than the *trans*-isomers. As mentioned by Gessner et al. in their computational study,[1] the thermodynamical properties of diaziridine derivatives are important for the modeling of high-energy materials; therefore, the investigation of DABH molecule has practical importance besides fundamental research.

In principle, the DABH molecule can form boat, chair, twist, and two half-chair conformations (see Chart 1). The conformation of a saturated ring depends on the balance between angle strain and torsional strain around the individual bonds and transannular interactions.[2–5] In the case of the DABH molecule, which contains nitrogen atoms with lone pairs, orbital interactions (anomeric effects) also influence the ring structure.[6] The conformational behavior of DABH has been studied in the past both experimentally, mainly by NMR spectroscopy, and theoretically. According to the results of ^{1}H and ^{13}C NMR spectroscopic investigations,[7] this molecule has a boat conformation (**1a**). On the other hand, the data from PE,[8,9] IR,[10] and ^{1}H NMR[9] spectroscopy, as well as results of AM1 calculations,[8] led the authors conclude that the DABH molecule possesses one of the possible half-chair conformations (**1c**, **1d**).

There are no structural data on free DABH molecules in the literature. To date, only one DABH derivative, 6,6′-bis(1,5-diazabicyclo[3.1.0]hexane) ((**2**), see Chart 2), has been studied by using gas-phase electron diffraction (GED).[11] It was shown that both DABH rings in this molecule have a boat conformation. Bicyclohexane (BH) is closely related to the DABH as a parent molecule in which nitrogen atoms are replaced by CH groups. The GED study[12] has showed that BH possesses a boat conformation. According to the Cambridge Structural Database,[13] only a few molecular structures of closely related DABH derivatives have been determined in the solid state (see Chart 2), namely, 6-phenyl-1,5-diazabicyclo(3.1.0)hexane (**3**),[14] 6-(4-methoxyphenyl)-1,5-diazabicyclo(3.1.0)hexane (**4**),[14] 6-(4-chlorophenyl)-1,5-diazabicyclo(3.1.0)hexane (**5**),[15] and already mentioned 6,6′-bis(1,5-diazabicyclo(3.1.0)hexane) (**2**).[16] In all these cases, the DABH moiety has a boat conformation. Despite the

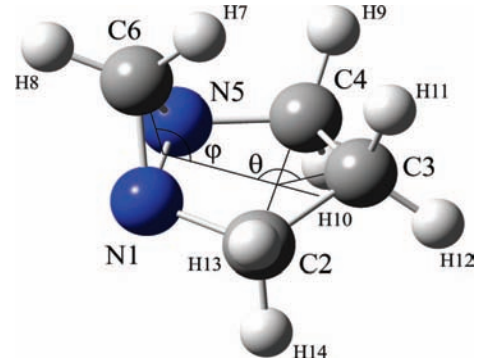

Figure 1. Atom-numbering scheme for the DABH molecule. The boat conformation is shown.

CHART 1: Conformations of the DABH Molecule[a]

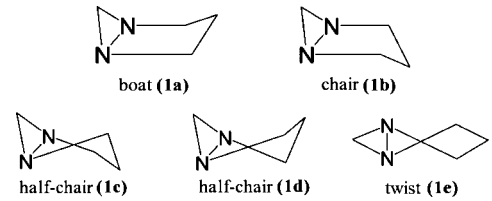

[a] Hydrogen atoms are not shown.

* Corresponding author. E-mail: yuri.vishnevskiy@gmail.com.
† University of Ulm.
‡ Moscow State University.
§ Russian Academy of Sciences.

10.1021/jp801346v CCC: $40.75
Published on Web 05/20/2008

CHART 2: Some of the DABH Derivatives[a]

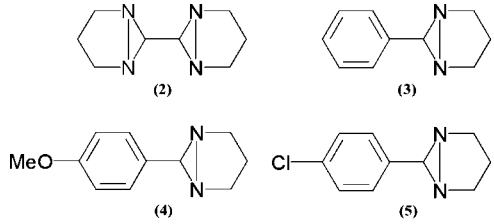

[a] Hydrogen atoms are not shown.

general usefulness of data on molecular structure in the crystal phase, they cannot be directly used as a good guide to conformational preference in a gas phase because of packing effects.[17]

The main objective of the work reported in this paper is to investigate geometrical structure and conformational composition of DABH by using the GED method augmented by quantum-chemical calculations and to understand the reasons of conformational stabilization. In addition, a quantum-chemical study of BH was performed in order to find out the similarities and differences between the BH and DABH structures and the factors of their conformational stabilization. DABH will thus contribute to the understanding of structure features and conformational properties of a *cis*-diaziridines.

Quantum-Chemical and Vibrational Calculations

The major part of quantum-chemical ab initio and density functional theory (DFT) investigations were performed with the Gaussian 03 program package[18] by using the popular three-parameter hybrid functional B3LYP[19] and MP2[20] theory with standard basis sets.

The following electronic configuration was considered in MP2 and B3LYP calculations: [core](5a′)^2(6a′)^2(3a″)^2(7a′)^2(4a″)^2(8a′)^2-(9a′)^2(10a′)^2(11a′)^2(5a″)^2(12a′)^2(13a′)^2(6a″)^2(7a″)^2(14a′)^2(15a′)^2-(8a″)^2. In order to save computational time, we used a frozen-core (FC) approximation in MP2, MP4, CISD, and CCSD methods; that is, six inner shells were excluded from the correlation calculation. This is a reasonable approximation for the case of DABH because the Mulliken population analysis[21] showed that the electron density of the first six molecular orbitals is perfectly localized on the inner 1s atomic orbitals of the corresponding C and N atoms. The energy gap between the last core and the first valence orbitals (9.9 au) confirmed the validity of the FC approximation. To check the applicability of the one-determinant MP2 and B3LYP methods for describing DABH geometrical and dynamical properties, we performed additional single-point CISD/cc-pVTZ energy calculation for the boat conformation by means of PC GAMESS program.[22] The obtained configuration interaction (CISD) wave function corresponding to the lowest energy contained the above-described configuration state function (CSF) with a coefficient of 0.907 (ca. 82%), whereas the coefficients for all other CSFs were less than 0.05. Thus, the ground electronic state of DABH is well described by a closed-shell single-determinant wave function. The MP2 natural occupied orbitals contain ca. 98% electrons as calculated by the MP2/cc-pVTZ approximation; this value is somewhat higher than the CISD result.

In a first step, the geometry optimizations of DABH were performed by the B3LYP and the MP2 methods with small 6-31G(d) basis set by using several nonsymmetric initial geometries approximately corresponding to all five possible conformations (see Chart 1). These computations were performed by using standard gradient techniques with tight-convergence criteria and the UltraFine-Grid option in the case of DFT calculations. The nature of each stationary point was checked by analytical calculation of harmonic vibrational frequencies. It was revealed that both B3LYP and MP2 methods give only three minima on a potential hypersurface corresponding to the twist conformation (C_2 symmetry) and to the boat and chair (both of C_s symmetry) conformations. The most stable conformation was the boat one, whereas the MP2 (B3LYP) relative energies for the chair and twist conformations were 3.78(3.65) and 49.54(48.31) kcal mol^{-1}, respectively. The values of the most important geometrical parameters for different conformers of DABH as calculated by the MP2/6-31G(d) method are summarized in Table 1. For the boat conformation, we performed additional geometry optimizations within the C_s-symmetry point group by MP2, MP4(SDQ), and CCSD methods paired with cc-pVTZ basis set. In order to check the influence of diffuse functions on the obtained geometrical parameters, we also performed MP2/aug-cc-pVTZ calculations. The calculated geometrical parameters of the boat conformer are given in Table 2.

TABLE 1: Most Important Geometrical Parameters (in Angstroms and Degrees) of DABH, Relative Energies, and Degrees of Strain as Calculated by the MP2/6-31G(d) Method

parameter	boat	chair	twist
(N1−N5)	1.515	1.542	1.581
(C6−N1)	1.452	1.450	1.432
(C2−N1)	1.480	1.486	1.458
(C2−C3)	1.533	1.527	1.576
(N1−C6−N5)	62.9	64.3	67.0
(C6−N1−N5)	58.5	57.9	56.5
(C6−N1−C2)	111.7	112.1	134.7
(N5−N1−C2)	107.0	106.3	93.6
(N1−C2−C3)	108.1	104.9	97.8
(C2−C3−C4)	101.9	102.0	103.4
φ	105.4	106.2	
θ	153.2	218.1	
τ^a			44.5
ΔA^b, deg	44.7	54.2	130.9
ΔE, kcal mol^{-1}	0.00	3.78	49.54
ΔG, kcal mol^{-1}	0.00	3.46	47.89

[a] Dihedral angle between the planes formed by atoms (N1−N5−C6) and (C2−C3−C4). [b] Degree of strain. See text for details.

The molecular structure and conformational stability of BH were studied by using the MP2 and the B3LYP methods with the 6-31G(d), 6-31G(d,p), and 6-31G(df,p) basis sets. According to these calculations, three stable conformations exist for this compound: boat (C_s), chair (C_s), and twist (C_2). The energy values and geometrical parameters of BH as obtained from MP2/6-31G(d) calculations are listed in Table 3. Other combinations of methods and basis sets give similar results.

In the second step, the potential-energy functions for boat−chair conformational conversion of DABH were calculated by geometry optimizations at several fixed angles θ with the RHF, B3LYP, and MP2 methods and the small 6-31G(d) basis set (see Figure 2). All calculations give global minimum corresponding to the boat conformation. The MP2 potential curve possess additional minimum corresponding to the chair conformation and barrier at $\theta \approx 195°$ and 4.6 kcal mol^{-1} above the boat form. The B3LYP potential curve formally has an additional very shallow minimum and a small barrier of about 0.1 kcal mol^{-1} above the chair form. In order to obtain a more reliable potential curve, we have used the MP2 method paired with a relatively large cc-pVTZ basis set. The obtained curve

TABLE 2: Most Important Geometrical Parameters of DABH (Boat Conformer) as Determined by the GED Method and Predicted by Quantum-Chemical Calculations[a]

		MP2, r_e,$\angle_e$			
parameter (Å, deg)	GED, r_e, $\angle_e$	cc-pVTZ	aug-cc-pVTZ	MP4(SDQ)/cc-pVTZ, r_e, $\angle_e$	CCSD/cc-pVTZ, r_e, $\angle_e$
N1−N5	1.506(13)	1.513	1.515	1.497	1.496
C6−N1	1.442(2)	1.448	1.449	1.443	1.444
C2−N1	1.469(4)	1.475	1.476	1.475	1.475
C2−C3	1.524(7)	1.530	1.531	1.533	1.533
$(C-H)_{av}$	1.100(5)	1.087	1.088	1.087	1.087
N5−N1−C2	107.7(4)	106.9	106.9	107.4	107.5
N1−C2−C3	106.5(9)[b]	108.2	108.1	107.9	109.9
C6−N1−C2	114.8(8)[b]	111.4	111.5	111.9	111.9
C2−C3−C4	104.0(10)[b]	101.6	101.8	101.8	101.8
N5−C6−N1	63.0[b,c]	63.0	63.0	62.5	62.4
φ	108.7(9)	106.9	105.1	105.5	105.5
θ	153.5(19)	152.9	152.9	153.8	154.0

[a] Error limits are estimated total errors, see text and Table 6 for details. [b] Dependent parameter. [c] Constrained value because r(N1−N5) and r(C6−N5) = r(C6−N1) were refined in one group.

TABLE 3: Most Important Geometrical Parameters (in Angstroms and Degrees) of BH, Relative Energies, and Degrees of Strain as Calculated by the MP2/6-31G(d) Method

parameter	boat	chair	twist
(C1−C5)	1.511	1.515	1.524
(C1−C6)	1.506	1.504	1.511
(C1−C2)	1.517	1.526	1.516
(C2−C3)	1.540	1.539	1.589
(C1−C6−C5)	60.2	60.4	60.6
(C6−C1−C5)	59.9	59.8	59.7
(C6−C1−C2)	117.4	117.2	144.6
(C5−C1−C2)	107.9	107.7	99.7
(C1−C2−C3)	104.5	104.4	98.6
(C2−C3−C4)	105.0	105.0	106.8
φ	111.8	111.7	
θ	148.7	212.5	
τ[a]			37.0
ΔA[b], deg	60.3	61.7	127.3
ΔE, kcal mol^{-1}	0.00	3.65	56.54
ΔG , kcal mol^{-1}	0.00	3.26	55.65

[a] Dihedral angle between the planes formed by atoms (C1−C5−C6) and (C2−C3−C4). [b] Degree of strain. See text for details.

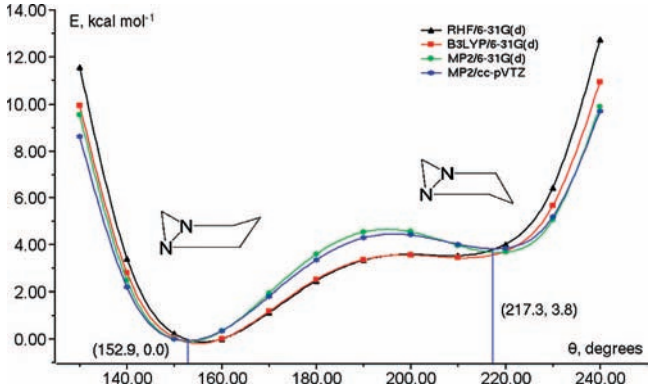

Figure 2. Potential functions of boat−chair conformational conversion of DABH. θ is the angle between the planes formed by (C2−N1−N5−C4) and (C2−C3−C4) groups of atoms. Vertical bars indicate positions of the minima of the MP2/cc-pVTZ curve.

(see Figure 2) is close to the MP2/6-31G(d) one. Figures S1 and S2 (Supporting Information) show the differences between geometrical parameters of DABH configurations with a fixed angle θ and the corresponding parameters of the most stable boat conformation as calculated by the MP2/cc-pVTZ method.

To gain insight into the conformational properties of the DABH, a natural bond orbital (NBO) analysis[23] was performed for all three possible conformations by using the B3LYP and the MP2 methods with the 6-31G(d), 6-31G(d,p), and 6-31G(d-f,p) basis sets. At the same levels of theory, we also performed geometry optimization and NBO analysis for the BH molecule in order to examine the reasons leading to the stabilization of the boat conformation. The stabilization energies of the orbital interactions as obtained from NBO analysis by using the B3LYP/6-31G(d) wave function are presented in Table 4. The other conbinations of methods and basis sets led to similar results. The NBO computations were performed by using the NBO 4.M program[24] within the PC GAMESS program package.

In order to better understand the reasons of conformational preference, we also calculated the ring strain of DABH and BH. The methods of conventional strain-energy[25] calculations, based on isodesmic models,[26] (hyper)homodesmotic models,[27–29] and so forth cannot be applied to explain the energy difference between several conformers of the same molecule. In our case, such computations would lead to values directly connected with the relative heats of formation of the conformers, which in turn, we want to explain. Instead, we used direct comparison of the geometrical parameters of the boat, chair, and twist conformers of DABH and BH with the corresponding parameters in reference strain-free molecules. The *cis*-*N*-methyl,*N*-ethyl-diaziridine (Figure 3), *cis*-1-methyl,2-ethyl-cyclopropane, and propane molecules were chosen for comparison. For these molecules, the geometry optimizations were performed at the same levels of theory as in the case of DABH and BH molecules. The obtained geometrical parameters are listed in Table S1 in the Supporting Information. The value of the reference (C−C−C) angle in the propane molecule is 112.4°, as calculated by MP2/6-31G(d). The degree of strain for each conformation was calculated as

$$\Delta A = \sum |\alpha_i^{\mathrm{conf}} - \alpha_i^{\mathrm{ref}}| \qquad (1)$$

where the summation is over all absolute values of the differences between angles in the DABH conformer and the corresponding ones in the reference molecules. This corresponds to the well-known Baeyer strain,[30] which seems to play the most significant role in DABH among other types of strain. The obtained values are presented in Tables 1 and 3.

To provide estimates of the amplitudes of vibrations and the curvilinear corrections, which are used in the gas-phase electron-diffraction refinements, the analytical quadratic and numerical

TABLE 4: Most Important Orbital Interaction Energies (kcal mol^{-1}) for the Boat, Chair, and Twist Conformers of DABH (X = N) and BH (X = C) as Derived from B3LYP/6-31G(d) wavefunctions[a]

	DABH			BH		
parameters	boat	chair	twist	boat	chair	twist
n(X1) → σ*(C2−C3)	4.02	1.15	1.05			
n(X1) → σ*(C4-X5)	2.08	1.90	<0.05			
n(X1) → σ*(C2−H13)	<0.05	1.57	7.00			
n(X1) → σ*(C2−H14)	1.13	1.69	0.62			
n(X1) → σ*(C6−H7)	3.62	3.61	7.89			
n(X1) → σ*(C6−H8)	1.51	1.44	2.71			
σ(X1−X5) → σ*(C2−C3)	0.53	0.76	1.80	0.44	0.55	1.52
σ(X1−X5) → σ*(X1−C6)	4.02	4.18	7.27	5.30	5.44	8.51
σ(X1−X5) → σ*(C2−H13)	2.13	1.23	<0.05	2.60	1.47	0.06
σ(X1−X5) → σ*(C2−H14)	<0.05	0.27	3.64	<0.05	0.28	3.87
σ(X1−X5) → σ*(C6−H7)	3.36	2.88	2.63	5.25	4.54	3.58
σ(X1−X5) → σ*(C6−H8)	1.93	2.20	2.63	1.83	2.13	3.58
σ(C2−H13) → σ*(C3−C4)	1.41	<0.05	0.09	1.84	<0.05	0.18
σ(C2−H13) → σ*(X1−X5)	3.32	1.16	<0.05	2.19	0.88	<0.05
σ(C2−H13) → σ*(C3−H12)	0.19	1.97	1.30	0.08	1.79	1.14
σ(C2−H14) → σ*(X1−C6)	3.70	2.16	2.34	4.09	2.08	2.20
σ(C2−H14) → σ*(C3−H11)	2.10	0.14	0.23	2.04	0.10	0.21
σ(C2−H14) → σ*(C3−C4)	<0.05	1.70	1.17	<0.05	1.81	1.28
σ(C2−C3) → σ*(X1−X5)	0.55	1.19	1.13	0.45	0.86	0.85
σ(C2−C3) → σ*(C4−H9)	1.84	0.12	0.94	1.61	0.12	0.75
σ(C2−C3) → σ*(C4−H10)	0.19	1.87	0.26	0.11	1.59	0.28
σ(C2−C3) → σ*(C4−X5)	1.23	1.09	0.98	0.37	0.39	0.34
σ(C3−H11) → σ*(C2−H14)	1.81	0.09	0.33	2.09	0.07	0.29
σ(C3−H11) → σ*(C2-X1)	<0.05	2.06	1.02	<0.05	1.69	1.08
σ(C3−H11) → σ*(C4−X5)	<0.05	2.06	<0.05	<0.05	1.69	0.16
σ(C3−H12) → σ*(C2−H13)	0.20	2.27	1.24	0.07	2.13	1.18
σ(C3−H12) → σ*(C2−X1)	1.94	<0.05	<0.05	1.70	<0.05	0.16
σ(C3−H12) → σ*(C4−X5)	1.94	<0.05	1.02	1.70	<0.05	1.08
ΔE_{tot},[b] kcal mol^{-1}	0.00	3.65	48.31	0.0	3.18	53.71
ΔE_{del},[c] kcal mol^{-1}	32.22	23.48	20.73	21.68	19.75	19.17
ΔE_{del},[d] kcal mol^{-1}	15.27	4.18	3.45			
ΔE_{del},[e] kcal mol^{-1}	20.62	19.23	40.62			

[a] Estimated energies by second-order perturbation theory analysis of Kohn−Sham matrix in NBO basis. Only symmetry-unique interactions are presented. n is the lone electron pair, σ is the bond orbital, and σ* is the antibonding orbital. The numeration for BH is the same as that for DABH. [b] Relative values of total energy. [c] Energy change by deletion of σ*(C2−C3) and σ*(C3−C4) antibonding orbitals. [d] Energy change by deletion of the off-diagonal elements of Kohn−Sham matrix in NBO basis, corresponding to the n(N1) → σ*(C2−C3) and n(N5) → σ*(C3−C4) interactions. [e] Energy effect of deletion of n(N1) → σ*(C2−C3), n(N5) → σ*(C3−C4), n(N1) → σ*(C2−H13), n(N1) → σ*(C2−H14), n(N5) → σ*(C4−H9), and n(N5) → σ*(C4−H10) interactions.

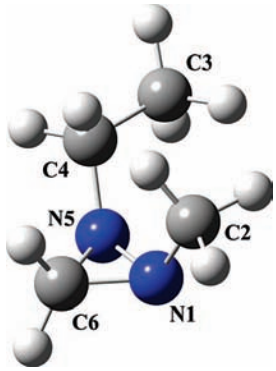

Figure 3. Atom numbering scheme for the *cis-N*-methyl,*N*-ethyldiaziridine molecule.

cubic force fields were calculated for the boat, chair, and twist conformations of DABH by the MP2/6-31G(d) and B3LYP/6-31G(df,p) methods. The boat conformer of this molecule belongs to the C_s symmetry and has 36 fundamental modes distributed as 21A′ + 15A″. The obtained harmonic vibrational frequencies, IR intensities, and Raman scattering activities and the approximate descriptions of the corresponding normal modes of the boat conformer are given in Table S2 in the Supporting Information. The B3LYP method produces generally lower values of the vibrational frequencies than does MP2 with the exception of ring deformation and twisting modes ν_{35} and ν_{36}. The mode ν_{21} with the lowest frequency of about 248 (B3LYP) and 275 (MP2) cm^{-1} corresponds to the ring puckering vibration. The calculations of shrinkage corrections $\Delta(r_e - r_a)$ to the equilibrium geometry and the mean-square amplitudes of vibrations l_{hl} were performed by using the SHRINK program.[31–34]

TABLE 5: Conditions of the Gas-Phase Electron Diffraction Experiment

parameter	short camera distance	long camera distance
nozzle-to-film distance, mm	193.8	362.2
accelerating voltage, kV	60.0	60.0
electron beam, μA	1.0	1.2
temperature, K	293.0	293.0
residual gas pressure, Torr	2.0×10^{-5}	4.0×10^{-5}
electron wavelength, Å	0.049930	0.497741
used s range, Å^{-1}	7.2−34.0	4.0−18.6
number of inflection points[a]	3	2
R_{exp}, %	5.5	5.4

[a] Number of inflection points on a background line.

Experimental Section

The DABH was synthesized and purified according to the methods described earlier.[15,35,36] Its purity was determined by iodometric titration to be more than 99%. The electron diffraction patterns were recorded by using the EG-100 M apparatus at the Moscow State University. The details of the experiment are presented in Table 5. The optical densities were obtained by using a calibrated Epson PERFECTION 4870 PHOTO scanner. The intensity curves were obtained by applying the method described elsewhere.[37] The sector function and electron wavelengths were estimated by using CCl_4 diffraction patterns, recorded along with the substance under investigation, by following a recently developed method.[38] The total intensity curves and background lines are shown in Figure S3 in the Supporting Information. The quality of experimental data was estimated by means of experimental R factors (R_{exp})[39] (see Table 5) for long and short camera distances.

Structural Analysis

Models of DABH. The structural analysis was performed by using the UNEX 1.5 program.[40] The three static models of the boat, chair, and twist conformers were tested. The geometry of each conformer was defined in a form of z-matrix. The C_s symmetry was assumed for the boat and chair models, and the C_2 symmetry was assumed for the twist model. In all the models, the following independent geometrical parameters were considered (see Figure 1): r(N1−N5), r(N1−C6), r(N5−C6), r(N1−C2), r(N5−C4), r(C2−C3), r(C3−C4), r(C6−H7), r(C6−H8), r(C4−H9), r(C4−H10), r(C3−H11), r(C3−H12), r(C2−H13), r(C2−H14), ∠(N1−N5−C4), ∠(N5−N1−C2), several ∠(C−C−H), and∠(N−C−H) and also φ and θ dihedral angles in the cases of boat and chair conformers. Because of the symmetry constraints and in order to avoid strong correlations, some of the geometrical parameters were separated into the following groups: (1) (N1−N5), four (C−N), and two (C−C) distances; (2) all (C−H) distances; and (3) two (N−N−C)

TABLE 6: Values of the Parameter Errors from Different Sources

parameter, Å, deg	3σ[c]	S_{err}[d]	Δ_{const}[e]	Δ_{vib}[f]	Δ_{bgl}[g]	Δ_{dyn}[h]	Δ_{tot}[l]
N1−N5	0.0009	0.0015	0.0133	0.0008	0.0004	0.0004	0.013
C6−N1	0.0009	0.0014	0.0014	0.0008	0.0004	0.0000	0.002
C2−N1	0.0009	0.0015	0.0036	0.0008	0.0004	0.0002	0.004
C2−C3	0.0009	0.0015	0.0065	0.0008	0.0004	0.0004	0.007
$(C-H)_{av}$	0.0043	0.0010	0.0037	0.0002	0.0002	−0.0002	0.005
N5−N1−C2	0.47	0.0	0.23	0.06	0.17	0.04	0.4
N1−C2−C3	1.16	0.0	0.39	0.09	0.53	−0.01	0.9
C6−N1−C2	0.99	0.0	0.56	0.35	0.57	−0.04	0.8
C2−C3−C4	1.39	0.0	0.67	0.19	0.50	0.13	1.0
φ(CNN)	1.14	0.0	0.59	0.42	0.58	0.07	0.9
θ(CCC)	1.57	0.0	1.72	0.86	0.54	1.00	1.9
11[a]	0.0016	0.0005	0.0007	0.0001	0.0001		0.0013
12[a]	0.0034	0.0006	0.0014	0.0001	0.0008		0.0025
13[a]	0.0111	0.0005	0.0100	0.0064	0.0038		0.0119
14[a]	0.0188	0.0008	0.0984	0.0142	0.0002		0.0990
ΔR_{str}[b], %			0.08	0.03	1.6		

[a] Corresponding groups of mean-square amplitudes from Table S3 in the Supporting Information. [b] Largest deviation of the total structural R factor. [c] 3-fold mean-square deviation as obtained from least-squares analysis. [d] Scale error calculated as $S_{err} = kp$, where p is the parameter value and k is 0.001 for distances and 0.01 for amplitudes. Scale error is zero for angles. [e] Effects of different geometrical constraints. Calculated as the largest absolute deviations of the final parameter values (see Tables 2 and S3 in the Supporting Information) and those which were obtained by using geometrical constraints from MP2/aug-cc-pVTZ, MP4(SDQ)/cc-pVTZ, and CCSD/cc-pVTZ calculations. [f] Effects of using different sets of mean-square amplitudes and shrinkage correction, calculated in the same manner as Δ_{const} by using additional set of amplitudes and corrections as calculated from B3LYP/6-31G(df,p) quadratic and cubic force fields. [g] Effects of increasing and decreasing the flexibility of backgrounds by changing the number of inflection points on a background spline function. [h] Effect of dynamical averaging of the geometrical parameters, calculated as the difference of the equilibrium and average values of the geometrical parameters along the potential curve obtained in MP2/cc-pVTZ computations. Average values were estimated as $p_{av} = \sum[p(\theta)\ \exp(-V(\theta)/RT)]/\sum[\exp(-V(\theta)/RT]$, where $p(\theta)$ and $V(\theta)$ are the optimized parameter value and potential energy of the structure with a fixed angle θ; the summations were performed for $130.0° \le \theta \le 200.0°$ with steps of 10.0°. [l] Total errors calculated as $\Delta_{tot} = (3(\sigma)^2 + (S_{err})^2 + (\max\{\Delta_{const},\Delta_{vib},\Delta_{bgl},|\Delta_{dyn}|\})^2)^{1/2}$.

angles. The differences between the parameter values within one group were fixed to the values resulting from the MP2/cc-pVTZ calculations (see Table 2). All other independent geometrical parameters were fixed to the MP2/cc-pVTZ values. Grouping the similar mean-square amplitudes together was performed for each model independently to avoid strong correlations. The starting values for all geometrical parameters were taken from the MP2/cc-pVTZ calculations. In the structural analysis, we tested two sets of mean-square amplitudes and curvilinear corrections as calculated from the B3LYP/6-31G(df,p) and the MP2/6-31G(d) quadratic and cubic force fields. For both sets, we obtained virtually identical agreement with the experimental intensities after parameter refinements. The final results were obtained by using the MP2/6-31G(d) force field. The total structural R factors (R_{str}) after parameter refinements for the boat, chair, and twist models were 5.0, 9.7, and 14.1%, respectively. Taking this into account and considering the relative energy values, we concluded that the boat conformer exists exclusively in a gas phase at temperatures of about 300 K. We did not try to refine the mixture of boat and chair conformers because the refinement of the most stable boat conformer has led to a satisfactory agreement between the experimental and calculated molecular intensities.

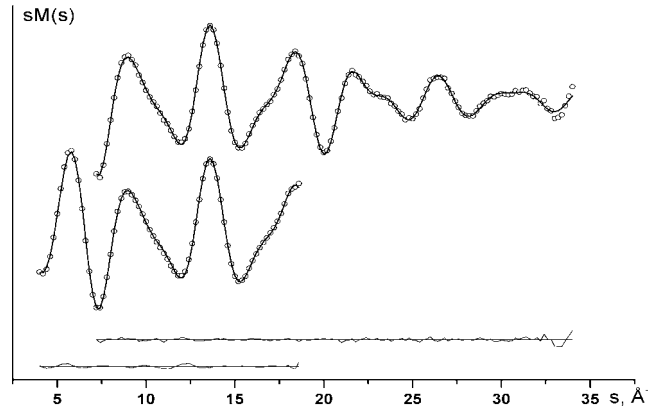

Figure 4. Molecular-intensity curves of DABH molecules and corresponding difference curves.

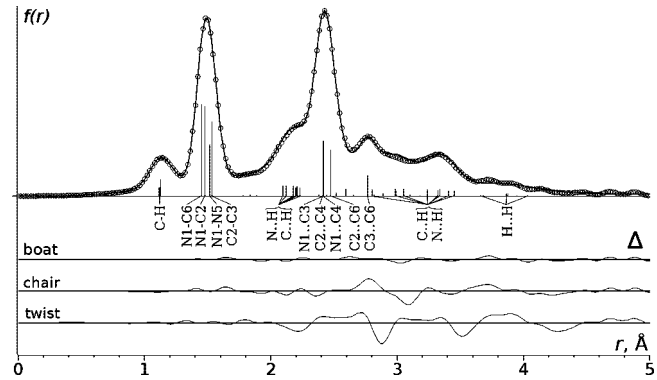

Figure 5. Experimental (open circles) and theoretical (full line) radial-distribution curves for DABH (boat conformer). Vertical bars indicate interatomic distances. The difference curves for all models are given at the bottom.

The experimental and theoretical molecular-intensity curves of the boat conformer along with the difference curves are shown in Figure 4. The resulting experimental geometrical parameters for the boat conformer together with the theoretically predicted values are given in Table 2. Table S3 in the Supporting Information shows the theoretical and experimental mean-square amplitudes. The largest correlations were mainly between some vibrational amplitudes (l), dihedral angles, and scale factors of the $sM(s)$ curves. The values for the correlation coefficients related to the pairs φ/l^b, l^a/S_S, and φ/θ were −0.81, 0.74, and −0.72, respectively. S_S is the scale factor of the $sM(s)$ curve from short nozzle-to-plate distance. For the definition of the grouped vibrational amplitudes l^a-l^b, see Table S3 in the Supporting Information. Radial distribution functions (Figure 5) were obtained by the *sin*-Fourier inversion of the experimental and theoretical $sM(s)$ curves multiplied by $\exp(-0.00064s^2)$.

Reliability of Results. The values of experimental factors R_{exp} (see Table 5), which indicate the reproducibility of the GED experimental data, can be used as a reference for assessing the relative values of the structural factors R_{str}. By comparing R_{str} and R_{exp} values with each other, we distinguish three different cases: (i) $R_{str} \gg R_{exp}$ means that the applied theoretical model is inappropriate and does not reproduce the experimental data, (ii) $R_{str} \ll R_{exp}$ means that the model reproduces experimental data unreliably, leading to questionable results, and (iii) $R_{str} \approx R_{exp}$ indicates the reliability of the considered model. The latter case is applicable to the model of boat conformer where the R_{str} values of 3.1 and 6.4% for the long and short camera distances, respectively, are close to the corresponding R_{exp} values of 5.4 and 5.5%.

The common practice in GED structural studies is to calculate the total errors of the parameters as a superposition of standard deviations obtained from least-squares analysis and the so-called scale error.[41] In order to increase the significance level, the obtained values are additionally multiplied by a some factor in the range 2.0−3.0. It is believed that the true parameter values lie in a ranges given by the obtained uncertainties with a significance level of 95−99%. However, there are many other sources of errors which are rarely examined in a structural studies but can strongly influence the obtained results. In this work, we have made an attempt to estimate some of them: (i) effect of quantum-chemical constraints, (ii) errors from mean-square amplitudes and shrinkage corrections, (iii) effect of the different ways for background subtraction, and (iv) errors of using a static model for molecular-scattering intensity. Table 6 summarizes the results of error analyses, which include the various effects of changing conditions of the structural refinement. Note that the R_{str} values were nearly unchanged upon such tests. It is clearly seen that in this particular study, the largest errors originated from using quantum-chemical constraints and the smallest ones from using a static model.

Discussion

DABH and BH Conformations. One of the most interesting feature of the DABH is its conformational properties. According to the results of our GED structural analysis, DABH exists as the boat conformation at temperatures of about 300 K. The total structural *R* factors of the chair and twist conformations are significantly larger, and thus, they can be sorted out. The high total-energy values for these conformers support the results of the structural analysis. The conformational preference of DABH is mainly determined by ring strain and orbital interactions. According to our calculations (see Table 1), the twist form is far more strained ($\Delta A = 130.9$) than the boat ($\Delta A = 44.7$) and chair ($\Delta A = 54.2$ degrees) ones. This fact explains the very high relative energy with respect to the boat and chair conformations. The same conclusion can be made for the twist conformer of BH (see Table 3). However, the scheme applied in this work for ring-strain estimation is very approximative, and the difference between ΔA values for the boat and chair forms can hardly be used to explain the occurrence of the boat form rather than the chair form. The ΔA values for the boat and chair conformations of BH are even closer to each other than in the case of DABH. On the other hand, the energy difference between the boat and chair conformers can be rationalized on the basis of NBO analysis. Table 4 summarizes the results of NBO analysis for all conformations of both DABH and BH. Among all the interactions, the most important ones for DABH are n(N1) → σ^*(C2−C3) and n(N5) → σ^*(C3−C4) (see Figure 6), which are known as anomeric effects. The second-order perturbation theory analysis of a Kohn−Sham matrix in the NBO basis predicts stabilization energies of 4.02 and 1.15 kcal mol^{-1} for each n(N) → σ^*(C−C) interaction in the boat and chair conformations, respectively. The exact energy effects of electronic delocalization with participation of σ^*(C−C) antibonding orbitals are calculated to be 32.22, 23.48, and 20.73 kcal mol^{-1} (see Table 4) for the boat, chair, and twist conformations, respectively. This is a good indication that the σ^*(C−C) orbitals play an important role in the stabilization of the DABH conformations. The deletion energy of a specific n(N) → σ^*(C−C) interaction is found to be 15.27 kcal mol^{-1} in the boat form but only 4.18 kcal mol^{-1} in the chair form, thus contributing strongly to stabilizing the boat conformation. This is in agreement with our hypothesis that the n(N) → σ^*(C−C) anomeric effect is the most significant among other stabilization factors in the boat conformation. However, from these values, it is also evident that there are other stabilization interactions which favor the chair conformation by 7.44 kcal mol^{-1} in total. These are mostly n(N1) → σ^*(C2−H13), n(N1) → σ^*(C2−H14), n(N5) → σ^*(C4−H9), and n(N5) → σ^*(C4−H10) interactions, as can be seen from the last row in Table 4. The picture of orbital interactions in BH is more complicated than that in DABH. It is hardly possible to distinguish one or two most important interactions leading to the preference of the boat conformation.

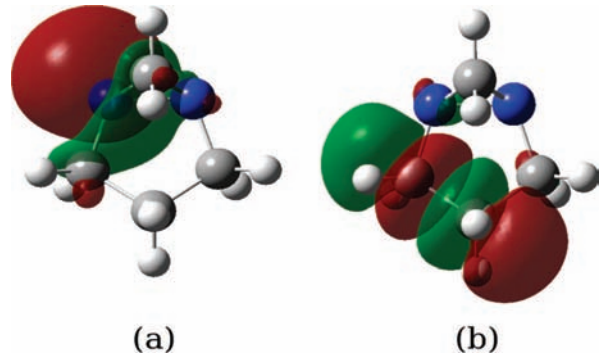

Figure 6. Natural orbitals, lone pair n(N1) (a) and antibond σ^*(C2−C3) (b) as produced by NBO analysis by using the wave function from the B3LYP/6-31G(d) calculation.

DABH Geometrical Parameters. Table 7 compares important skeletal parameters of DABH with those in some related molecules studied in both gas and crystal phase. It is also interesting to compare the obtained geometrical parameters with the corresponding ones in *trans-N,N*-dimethyldiaziridine (DMDA, **6**) and 1,2-dimethylhydrazine (DMH, **7**) molecules (see Chart 3). The parameters of these molecules are also presented in Table 7. The N−N bond length in the DABH is significantly larger than that in the DMH by 0.077 Å and close to the values in other DABH derivatives, in both gas and crystal phase. As expected, the geometry of DMH does not follow the general trends in diaziridines. It is interesting to note that the N−N bond length in DABH, which is a *cis*-diaziridine derivative, is very close to the corresponding value in the *trans*-DMDA. Thus, the N−N bond is not sensible to the *cis*−*trans* isomerization. However, as predicted by quantum-chemical calculations, its length may strongly depend on the ring conformation (see Table 1 and Figure S1 in the Supporting Information). All C−N distances in DABH are in very good agreement with the corresponding parameters in all other listed molecules except in DMH. In contrast, the C−C bonds diverge more significantly than the C−N bonds. The experimental C−H bond lengths are ill-conditioned parameters and seem to be somewhat overestimated. All angles in DABH are in accordance with those in the gas-phase structure of Bis-DABH (**2**) and solid-state structures of several DABH derivatives.

Reliability of Quantum-Chemical Methods. In general, the DFT and MP2 calculations provide correct results, indicating the boat conformation as the most stable. Both of these methods also predict very high energy twist conformation. In contrast to DFT, the MP2 method predicts the chair conformation to be 3.8 kcal mol^{-1} above the boat form. According to GED structural analysis, there is no evidence that the chair conformation exists in a gas phase at temperatures of about 300 K. However, this fact neither confirms nor contradicts the result of MP2 calculations because the population of the chair conformation would be very low at the temperature of the GED experiment (0.26%) to be reliably determined.

TABLE 7: Skeletal Geometric Parameters of DABH and Related Molecules

	GED				X-ray [a]			
parameters, Å, deg	DABH (**1**) this work, r_g, $\angle_e$	DMDA (**6**),[42] r_g, $\angle_\alpha$	DMH[b] (**7**),[43] r_g, $\angle_z$	bis-DABH (**2**),[11] r_g, $\angle_\alpha$	(**2**),[16] r_α, $\angle_\alpha$	(**3**),[14] r_α, $\angle_\alpha$	(**4**),[14] r_α, $\angle_\alpha$	(**5**),[15] r_α, $\angle_\alpha$
(N1−N5)	1.518(13)	1.514(6)	1.441(2)	1.511(2)	$(1.517)_{av}$	1.494	1.505	1.517
(C6−N1)	1.453(2)	1.448(2)		1.452(2)	$(1.449)_{av}$	$(1.455)_{av}$	$(1.451)_{av}$	$(1.457)_{av}$
(C2−N1)	1.479(4)		$1.463(9)_{av}$	1.483(2)	$(1.483)_{av}$	$(1.474)_{av}$	$(1.480)_{av}$	$(1.486)_{av}$
(C2−C3)	1.535(5)			1.543(2)	$(1.515)_{av}$	$(1.523)_{av}$	$(1.515)_{av}$	$(1.532)_{av}$
(C6−N1−C2)	114.8(8)	114.7(7)		111.1(16)	$(111.8)_{av}$	$(112.6)_{av}$	$(112.5)_{av}$	$(111.4)_{av}$
(N5−N1−C2)	107.7(4)	108.5(6)	$112.0(12)_{av}$	107.5[c]	$(106.6)_{av}$	$(107.3)_{av}$	$(106.9)_{av}$	$(107.1)_{av}$
(N1−C2−C3)	106.5(9)			107.6(11)	$(108.6)_{av}$	$(107.9)_{av}$	$(108.2)_{av}$	$(107.9)_{av}$
(C2−C3−C4)	104.0(10)			102.8[c]	$(102.6)_{av}$	102.4	102.6	102.5
φ	108.7(9)			104.5[c]	$(105.7)_{av}$	107.0	107.1	104.8
θ	153.5(19)			154.5[c]	$(154.6)_{av}$	153.9	154.5	153.3

[a] Data retrieved from the Cambridge Structural Database.[13] [b] Parameters for the most stable conformation are given. [c] Parameter was given without error limits. [av] Average value.

CHART 3: Molecules of *trans*-*N*,*N*-Dimethyldiaziridine and *N*,*N*-Dimethylhydrazine[a]

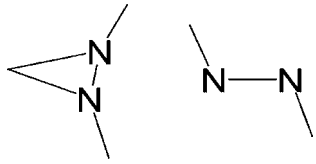

(6) (7)

[a] Hydrogen atoms are not shown.

The experimental geometrical parameters of DABH can be directly compared (see Table 2) with those from theoretical calculations because of the applied $\Delta(r_e - r_a)$ corrections in the GED structural analysis. All parameters agree well between each other; however, the MP4 and CCSD methods give shorter N−N bonds than the MP2 method. The MP4(SDQ) and CCSD geometries are very close to each other. It is of interest to note that the augmented diffuse functions do not influence significantly the resulting geometrical parameters because the MP2 method produces very similar structures when paired with the cc-pVTZ and aug-cc-pVTZ basis sets.

Conclusions

A complete investigation of the gas-phase molecular structure of DABH was carried out by using the electron-diffraction technique complemented by theoretical methods. The experimental data shows that this molecule has a boat conformer. This is in agreement with quantum-chemical calculations which, however, predict two more stable conformations, chair and twist, with relative energies of about 3.8 and 50 kcal mol^{-1} above the boat form, respectively. These conformations are unobservable at the temperature of our GED experiment. The twist conformation is far more strained than the boat and chair ones. The NBO analysis has shown that the boat conformation is mostly stabilized by the anomeric $n(N) \rightarrow \sigma^*(C-C)$ interactions. There is good agreement between the geometry obtained in our GED investigation and the one calculated by the MP2, MP4, and CCSD methods.

Acknowledgment. This work was supported by the Russian Foundation of Basic Research (RFBR), Grant no. 05-03-32445, and the Dr. B. Mez-Starck Foundation (Germany).

Supporting Information Available: Calculated geometrical parameters of the *cis*-*N*-methyl,*N*-ethyl-diaziridine and *cis*-1-methyl,2-ethyl-cyclopropane; calculated vibrational frequencies, IR intensities, Raman scattering activities, and approximate descriptions of the normal modes; amplitudes of vibrations and vibrational corrections; DABH geometrical parameters relaxation; DABH total intensities and background lines. This material is available free of charge via the Internet at http://pubs.acs.org.

References and Notes

(1) Gessner, K. J.; Ball, D. W. *J. Mol. Struct.: THEOCHEM* **2005**, *730*, 95.
(2) Pitzer, K.; Donath, W. E. *J. Am. Chem. Soc.* **1959**, *81*, 3213.
(3) Romers, C.; Altona, C.; Buys, H. R.; Havinga, E. *Top. Stereochem.* **1969**, *4*, 39.
(4) Fuchs, B. *Top. Stereochem.* **1978**, *10*, 1.
(5) Greenberg, A.; Liebman, J. F. *Strained Organic Molecules*; Academic Press: New York, 1978.
(6) Kirby, A. J. *The Anomeric Effect and Related Stereochemical Effect at Oxygen*; Springer: Berlin, 1983.
(7) Shustov, G. V.; Denisenko, S. N.; Chervin, I. I.; Asfandiarov, N. L.; Kostyanovsky, R. G. *Tetrahedron* **1985**, *41*, 5719.
(8) Denisenko, S. N.; Kaupp, G.; Bittner, A. J.; Rademacher, P. *J. Mol. Struct.* **1990**, *240*, 305.
(9) Rademacher, P.; Koopman, H. *Chem. Ber.* **1975**, *108*, 1557.
(10) Koopman, H.-P.; Rademacher, P. *Spectrochim. Acta* **1976**, *32A*, 157.
(11) Atavin, E. G.; Golubinskii, A. V.; Popik, M. V.; Kuznetsov, V. V.; Makhova, N. N.; Vilkov, L. V. *J. Struct. Chem.* **2003**, *44*, 779.
(12) Shen, Q.; Mastryukov, V. S.; Boggs, J. E. *J. Mol. Struct.* **1995**, *352/353*, 181.
(13) Allen, F. H. *Acta Crystallogr.* **2002**, *B58*, 380.
(14) Molchanov, A. P.; Sipkin, D. I.; Koptelov, Yu. B.; Kopf, J.; Kostikov, R. R. *Zh. Org. Khim.* **2003**, *39*, 1410. (in Russian)
(15) Kuznetsov, V. V.; Kutepov, S. A.; Makhova, N. N.; Lyssenko, K. A.; Dmitriev, D. E. *Russ. Chem. Bull.* **2003**, *52*, 665.
(16) Kuznetsov, V. V.; Makhova, N. N.; Dekaprilevich, M. O. *Russ. Chem. Bull.* **1999**, *48*, 617.
(17) Bürgi, H. B. *Acta Crystallogr. A* **1998**, *54*, 873.
(18) Frisch, M. J.; Trucks, G. W.; Schlegel, H. B.; Scuseria, G. E.; Robb, M. A.; Cheeseman, J. R.; Montgomery, J. A., Jr.; Vreven, T.; Kudin, K. N.; Burant, J. C.; Millam, J. M.; Iyengar, S. S.; Tomasi, J.; Barone, V.; Mennucci, B.; Cossi, M.; Scalmani, G.; Rega, N.; Petersson, G. A.; Nakatsuji, H.; Hada, M.; Ehara, M.; Toyota, K.; Fukuda, R.; Hasegawa, J.; Ishida, M.; Nakajima, T.; Honda, Y.; Kitao, O.; Nakai, H.; Klene, M.; Li, X.; Knox, J. E.; Hratchian, H. P.; Cross, J. B.; Bakken, V.; Adamo, C.; Jaramillo, J.; Gomperts, R.; Stratmann, R. E.; Yazyev, O.; Austin, A. J.; Cammi, R.; Pomelli, C.; Ochterski, J. W.; Ayala, P. Y.; Morokuma, K.; Voth, G. A.; Salvador, P.; Dannenberg, J. J.; Zakrzewski, V. G.; Dapprich, S.; Daniels, A. D.; Strain, M. C.; Farkas, O.; Malick, D. K.; Rabuck, A. D.; Raghavachari, K.; Foresman, J. B.; Ortiz, J. V.; Cui, Q.; Baboul, A. G.; Clifford, S.; Cioslowski, J.; Stefanov, B. B.; Liu, G.; Liashenko, A.; Piskorz, P.; Komaromi, I.; Martin, R. L.; Fox, D. J.; Keith, T.; Al-Laham, M. A.; Peng, C. Y.; Nanayakkara, A.; Challacombe, M.; Gill, P. M. W.; Johnson, B.; Chen, W.; Wong, M. W.; Gonzalez, C.; Pople, J. A. *Gaussian 03*, revision D.02; Gaussian, Inc.: Wallingford, CT, 2003.
(19) Becke, A. D. *J. Chem. Phys.* **1993**, *98*, 5648.
(20) Møller, C.; Plesset, M. S. *Phys. Rev.* **1934**, *46*, 618.
(21) Mulliken, R. S. *J. Chem. Phys.* **1955**, *23*, 1833.

(22) Granovsky, A. A. PC GAMESS, version 7.1; http://classic-.chem.msu.su/gran/gamess/index.html.
(23) Foster, J. P.; Weinhold, F. *J. Am. Chem. Soc.* **1980**, *102*, 7211.
(24) Glendening, E. D.; Badenhoop, J. K.; Reed, A. E.; Carpenter, J. E.; Weinhold, F. *NBO 4.M*; Theoretical Chemistry Institute, University of Wisconsin: Madison, WI, 1999.
(25) Cox, J. D.; Pilcher, G. *Thermochemistry of Organic and Organometallic Compounds*; Academic Press: New York, 1970.
(26) Dill, J. D.; Greenberg, A.; Liebman, J. F. *J. Am. Chem. Soc.* **1979**, *101*, 6814.
(27) George, P.; Trachtman, M.; Bock, C. W.; Brett, A. M. *Tetrahedron* **1976**, *32*, 317.
(28) Hess, B. A.; Schaad, L. J. *J. Am. Chem. Soc.* **1983**, *105*, 7500.
(29) Blahous III, C.; Schaefer III, H. F. *J. Phys. Chem.* **1988**, *92*, 959.
(30) Baeyer, A. *Ber. Dtsch. Chem. Ges.* **1885**, *18*, 2269.
(31) Sipachev, V. A. *J. Mol. Struct.: THEOCHEM* **1985**, *121*, 143.
(32) Sipachev, V. A. In *Advances in Molecular Structure Research*; Hargittai, I., Hargittai, M. Eds.; JAI Press: Stamford, 1999; pp 263−311.
(33) Sipachev, V. A. *Struct. Chem.* **2000**, *11*, 167.
(34) Sipachev, V. A. *J. Mol. Struct.* **2004**, *693*, 235.
(35) Ohme, R.; Schmits, E.; Dolge, P. *Chem. Ber.* **1966**, *99*, 2104.
(36) Ger. Pat. 3607993, 1987; Chem. Abstrs. **1987**, *107*, 236687h.
(37) Vishnevskiy, Yu. V. *J. Mol. Struct.* **2007**, *833*, 30.
(38) Vishnevskiy, Yu. V. *J. Mol. Struct.* **2007**, *871*, 24.
(39) Vishnevskii, Y. V.; Shishkov, I. F.; Khristenko, L. V.; Rykov, A. N.; Vilkov, L. V.; Oberhammaer, H. *Russ. J. Phys. Chem.* **2005**, *79*, 1537.
(40) Vishnevskiy, Yu. V. UNEX 1.5; http://molstruct.chemport.ru/mykced_en.html.
(41) (a) Hargittai, I. In *Stereochemical Applications of Gas-phase Electron Diffraction. Part A. The Electron Diffraction Technique*; Hargittai, I., Hargittai, M. Eds.; VCH Publishers: New York, 1988, pp 1−54, Chapter 1. (b) Bartell, L. S. In *Stereochemical Applications of Gas-phase Electron Diffraction. Part A. The Electron Diffraction Technique*; Hargittai, I., Hargittai, M. Eds.; VCH Publishers: New York, 1988, pp 55−84, Chapter 2.
(42) Atavin, E. G.; Golubinskii, A. V.; Popik, M. V.; Kuznetsov, V. V.; Makhova, N. N.; Anikeeva, A. V.; Vilkov, L. V. *J. Struct. Chem.* **2003**, *44*, 784.
(43) Yamanouchi, K.; Sugie, M.; Takeo, H.; Matsumura, C.; Nakata, M.; Nakata, T.; Kuchitsu, K. *J. Phys. Chem.* **1987**, *91*, 823.

JP801346V